Nuclear rotation at the fission limit in math xmlns="http://www.w3.org/1998/Math/MathML">mmultiscripts>mi>Rf/mi>mprescripts>/mprescripts>none>/none>mn>254/mn>/mmultiscripts>/math>

D. Seweryniak, T. Huang, K. Auranen, A. D. Ayangeakaa, B. B. Back, M. P. Carpenter, P. Chowdhury, R. M. Clark, P. A. Copp, Z. Favier, K. Hauschild, X.-T. He, T. L. Khoo, F. G. Kondev, A. Korichi, T. Lauritsen, J. Li, C. Morse, D. H. Potterveld, G. Savard, S. Stolze, J. Wu, J. Zhang, and Y.-F. Xu

Phys. Rev. C **107**, L061302 — Published 9 June 2023

DOI: 10.1103/PhysRevC.107.L061302

Nuclear rotation at the fission limit in ^{254}Rf

D. Seweryniak,[1,*] T. Huang,[1,2] K. Auranen,[1] A.D. Ayangeakaa,[3,4] B.B. Back,[1] M.P. Carpenter,[1] P. Chowdhury,[5] R.M. Clark,[6] P.A. Copp,[1] Z. Favier,[7] K. Hauschild,[8] X.-T. He,[9] T.L. Khoo,[1] F.G. Kondev,[1] A. Korichi,[8] T. Lauritsen,[1] J. Li,[1] C. Morse,[6] D.H. Potterveld,[1] G. Savard,[1] S. Stolze,[1] J. Wu,[1] J. Zhang,[10] and Y.-F. Xu[9]

[1] *Argonne National Laboratory, Argonne, IL 60439, USA*
[2] *Institute of Modern Physics, Chinese Academy of Sciences, Lanzhou 730000, China*
[3] *University of North Carolina, Chapel Hill, North Carolina 27599, USA*
[4] *Triangle Universities Nucelar Laboratory, Duke University, Durham, North Carolina 27708, USA*
[5] *University of Massachusetts, Lowell, MA 01854, USA*
[6] *Lawrence Berkeley National Laboratory, Berkeley, CA 94720*
[7] *CEA, Département de Physique Nucléaire, Université Paris-Saclay, 91191, Gif-sur-Yvette, France.*
[8] *CNRS, IJCLab, Université Paris-Saclay, 91405, Orsay, France.*
[9] *College of Materials Science and Technology, Nanjing University of Aeronautics and Astronautics, Nanjing 210016, China*
[10] *College of Physics, Nanjing University of Aeronautics and Astronautics, Nanjing 210016, China*
(Dated: April 5, 2023)

A ground-state rotational band in the fissile nucleus ^{254}Rf was observed for the first time. Levels up to spin $14\hbar$ and excitation energy of 1.56 MeV were observed. The ^{254}Rf nuclei were produced using the ^{206}Pb(^{50}Ti,2n) fusion-evaporation reaction. It is the weakest reaction channel ever studied using in-beam γ-ray spectroscopic methods. The reaction products were separated from the beam in the Argonne Gas-Filled Analyzer. The ^{254}Rf nuclei were implanted into a double-sided Si strip detector at the AGFA focal plane and tagged with subsequent ground-state spontaneous fission decays using temporal and spatial correlations. Prompt γ rays in coincidence with the ^{254}Rf recoils were detected in the Gammasphere array of Ge detectors. In order to identify the ground-state rotational band in ^{254}Rf, a novel method for identifying rotational bands in low statistics γ-ray spectra was developed. The deduced ^{254}Rf kinematic moment of inertia is smaller compared to neighboring even-even nuclei. This is most likely associated with a slightly lower quadrupole deformation and stronger pairing correlations in ^{254}Rf. The behavior of the moment of inertia as a function of rotational frequency is similar to that of the lighter N=150 isotones ^{250}Fm and ^{252}No.

Introduction. The quest for super-heavy nuclei (SHN) is one of the frontiers of nuclear physics. In recent years, SHN with atomic numbers 113-118 have been discovered [1–3]. However, because of very small production cross sections, only the basic properties such as the dominant decay modes and the lifetimes are known for SHN. On the other hand, trans-fermium nuclei located near the deformed energy gaps Z=100 and N=152, which similarly to the heaviest nuclei owe their existence to shell corrections, can be produced with sufficiently large cross sections to facilitate spectroscopic studies. These nuclei are among the best rotors known and are an excellent testing ground for models which are used to describe the heaviest nuclei. One of the goals of nuclear theory is to predict the location and the magnitude of major spherical shell gaps which can determine the possible occurrence of the "island of stability" of SHN. However, different theoretical approaches do not agree (see Ref. [4] and references therein). For example, the microscopic-macroscopic approach predicts Z=114 and N=184 whereas various self-consistent calculations give different results. In particular, the Hartree-Fock method with Skyrme forces favors Z=126, N=184 while the relativistic mean field theory prefers Z=120 and N=172. It is worth noting that only the microscopic-macroscopic approach reproduces the Z=100, N=152 deformed shell gaps which have already been established experimentally. Interestingly, some of the orbitals which determine the spherical magic numbers for super-heavy nuclei are located close to the Fermi surface in the trans-fermium region.

Nuclei near Z=100, N=152 have been studied using in-beam, isomer and decay spectroscopic methods. See the recent review [5] of the experimental and theoretical developments in this mass region. In particular, in-beam spectroscopy has provided information about moments of inertia as a function of rotational frequency. The nuclear moment of inertia depends on deformation. However, because nucleons are paired, its value is lower than that for the rigid body and it only approaches the rigid body limit as the pairing correlations diminish. Pairing correlations depend on details of single-particle levels near the Fermi surface. In nuclei with closed shells, pairing correlations are weaker due to a lower density of states and increase as one departs from closed shells. Also, the moment of inertia undergoes a gradual rise at low rotational frequencies followed by a rapid increase when a pair of nucleons occupying an orbital with a high angular momentum breaks up and the unpaired nucleons align their angular momenta with the rotational axis of the core. In the Z=100, N=152 region the neutron $\nu j_{15/2}$ and/or the proton $\pi i_{13/2}$ pairs tend to align first [6]. The latter orbital is located near the Fermi surface in the heaviest nuclei.

Rotational properties of trans-fermium nuclei have been described within various theoretical frameworks. For example, their deformation and moments of inertia as well as the underlying single-particle structure were discussed using the macroscopic-microscopic approach with the Woods-Saxon potential and the Universal set of parameters in Ref. [7]. Furthermore, results of self-consistent mean field calculations with the SLy4 interaction and a density-dependent pairing force were presented in Ref. [8], while the Covariant Density Functional theory was used in Ref. [9] to calculate moments of inertia. The impact of higher order deformation on moments of inertia was discussed in Refs. [10] and [11] using the Total-Routhian Surface with the Cranking Shell Model and the Particle-Number-Conserving Cranking Shell Model, respectively.

Fission plays an important role in the realm of superheavy nuclei. It determines their production cross sections and it ultimately defines the limits of their existence. The ^{254}Rf ground state disintegrates rapidly by spontaneous fission with the shortest measured fission lifetime. The published ^{254}Rf half-life values have shown a wide variation, ranging from 500(200) μs in Ref. [12], 23(3) μs [13], and 29.6(+0.7-0.6) μs [14] until the value of 23.2(1.1) μs was measured recently [15] in agreement with Ref. [13]. In addition, two isomers were observed in this nucleus with half-lives of 4.7(1.1) μs and 247(73) μs [15]. They were interpreted as a 2-quasiparticle (qp) and a 4-qp K-isomer, respectively. Surprisingly, the half-life of the 2-qp isomer in ^{254}Rf is four orders of magnitude shorter than for the equivalent 2-qp isomers in the lighter N=150 isotones ^{250}Fm and ^{252}No. Currently, the reason for this abrupt change is not well understood. Despite the rapidly fissioning ground state, no fission events were observed for either of the two isomers. This implies that fission is hindered by a factor of at least 2 for the 2-qp isomer and by a factor of at least 25 for the 4-qp isomer compared to the ground-state fission. Superheavy nuclei with Z>118 are expected to decay rapidly by spontaneous fission and fission hindrance in isomeric states could be a possible mechanism for their survival. Another interesting aspect of rotation in the proton-rich trans-fermium nuclei is the interplay between fission and rotation at high spin. This interplay has been extensively discussed in Ref. [16] and in Ref. [17] for the case of ^{254}No. In ^{254}Rf, fission is expected to compete with γ decay at lower excitation energies than in ^{254}No due to a lower fission barrier. At present, the ^{256}Rf nucleus is the heaviest nucleus which has been studied using in-beam spectroscopic methods [18]. The ground-state rotational band in ^{256}Rf has been delineated up to spin $20\hbar$. Ground-state rotational bands are also known in the lighter N=150 even-even isotones ^{250}Fm [19] and ^{252}No [20] as well as in ^{254}No [21].

In order to trace the evolution of rotational properties away from the Z=100 and N=152 shells and to elucidate the role of a lower fission barrier, a search for γ-ray transitions in the fissile nucleus ^{254}Rf was carried out. This paper reports first observation of the ground-state rotational band in ^{254}Rf.

Experimental Details. ^{254}Rf nuclei were synthesized using the ^{206}Pb(^{50}Ti,2n) reaction. The cross section for this reaction is only 2.4(2) nb [13] which is almost a factor of 7 smaller compared to the production of ^{256}Rf [18]. A ^{50}Ti beam with an energy of 244 MeV delivered by the ATLAS linear accelerator at the Argonne National Laboratory impinged on 0.5 mg/cm^2-thick ^{206}Pb targets isotopically enriched to 95.9%. A 40μg/cm^2-thick and 10μg/cm^2-thick carbon layer was evaporated on the front and on the back of the targets, respectively. The experiment was performed in two parts. The targets were mounted on a wheel which rotated with a frequency of about 1200 rpm. During the first part, four 9 mm-wide target segments formed a circle with 17 mm average radius. Larger 11 mm-wide segments, which formed a 34 mm-radius circle, were used during the second part. The beam was wobbled horizontally with 5 Hz frequency to cover the whole target area. In total, the targets were irradiated for 94(84)h and the average beam intensity was about 20(25) pnA during the first (second) part. The beam was periodically swept away to avoid hitting the target wheel spokes. During the first part of the experiment the targets suffered significant damage and had to be replaced multiple times. This was attributed to bursts in beam intensity associated with the volatile nature of the sputtering process used to introduce the beam material into the plasma of the ion source. This problem was remedied by using larger targets during the second experiment.

Prompt γ rays were detected using Gammasphere, an array of Ge detectors arranged symmetrically around the target wheel. Gammasphere consisted of 65 and 70 detectors at the time of the first and the second part of the experiment, respectively. The average γ-ray energy resolution at energies between 100 keV and 500 keV was FWHM$\approx$3 keV. The reaction products recoiling from the target were separated from the beam in the Argonne Gas-Filled Analyzer (AGFA). AGFA consists of a large bore vertically-focusing quadrupole magnet and a combined-function horizontally-focusing magnetic dipole. AGFA was filled with He gas at 0.5 Torr and was set to transport reaction products centered around Bρ=2.08 Tm. After passing through the Parallel-Grid Avalanche Counter (PGAC) located at the exit from AGFA the reaction products were implanted into a 300-μm-thick 64x64 mm^2 double-sided Si strip detector (DSSD). The front and back side of the DSSD were divided into 160 strips each which were mutually orthogonal resulting in 25600 pixels. The DSSD energy resolution for α particles with energies around 5 MeV was FWHM$\approx$25 keV. An array of eight 4x7cm^2 300μm-thick single-sided Si strip detectors in a tunnel geometry was installed in front of the DSSD to catch escaping decay particles. Each detector

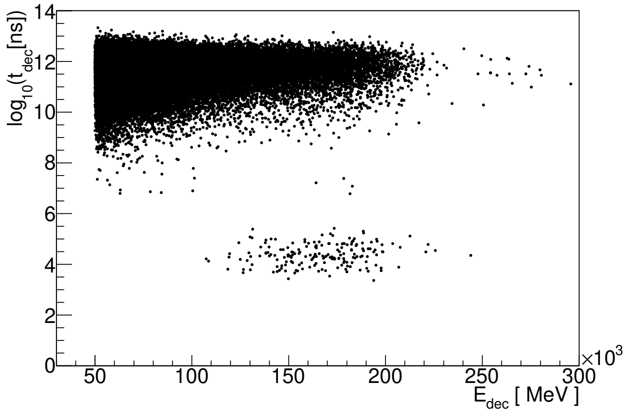

FIG. 1. Energies of decay events with energies larger than 50 MeV as a function of time with respect to preceeding implants. The log base 10 of the decay time expressed in nanoseconds is shown on the ordinate axis.

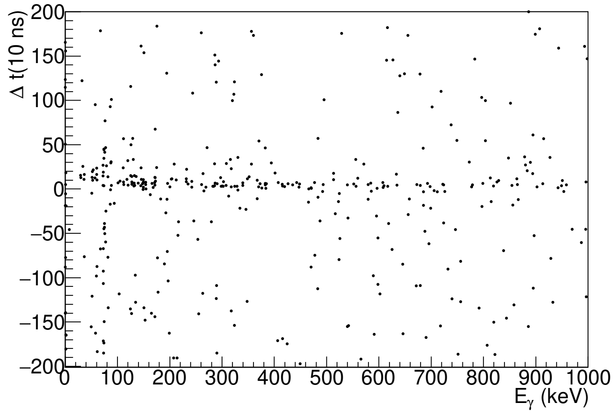

FIG. 2. Energies of γ rays correlated with ^{254}Rf fission decays as a function of the time beetween the γ rays and the implants.

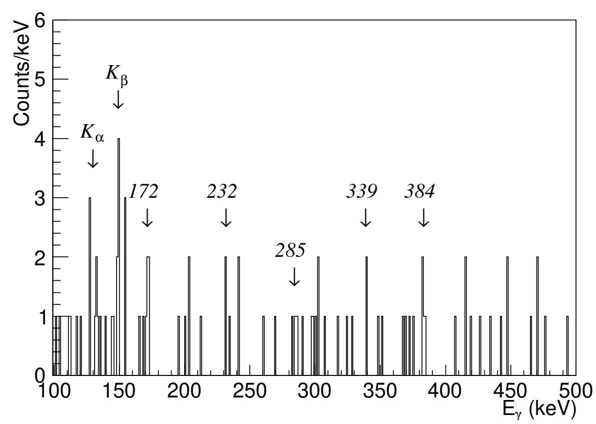

FIG. 3. Energy spectrum of γ rays in prompt coincidence with ^{254}Rf implants.

was divided into 7 strips perpendicular to the DSSD. A large area 5x5 cm^2 300 μm-thick Si detector was placed behind the DSSD to veto energetic light particles like protons and He atoms which punched through the DSSD. All events registered in the DSSD in coincidence with the PGAC were flagged as potential recoils and the remaining ones as potential decays. The energy deposited in the DSSD and the time of flight between the PGAC and the DSSD were used to suppress scattered beam events.

Results. Fig. 1 shows the energy spectrum of decay events as a function of the time with respect to preceding recoil events. A group of decay events with energies between 100 and 250 MeV corresponding to decay times around 20 μs is clearly separated from randomly correlated background decay events in Fig. 1. This group was interpreted as ^{254}Rf ground-state fission events. Four high-energy events with lifetimes around 10 ms correspond most likely to spontaneous fission of ^{256}Rf which was produced on ^{208}Pb contaminant present in the targets. In Fig. 2, energies of prompt γ rays detected in coincidence with ^{254}Rf recoils as a function of time between γ rays and implants are shown. A band of events corresponding to prompt coincidences is clearly visible in Fig. 2. Fig. 3 contains the spectrum of γ rays in prompt coincidence with the ^{254}Rf implants. Excess of counts at the energies corresponding to Rf K_α and K_β X-ray lines confirms assignment of the spectrum to ^{254}Rf. Clusters of counts at higher energies correspond to discrete transitions of the ground-state rotational band in ^{254}Rf. Guided by the known rotational bands in neighboring even-even nuclei, the group of 5 counts at 172 keV was interpreted as the $6^+ \rightarrow 4^+$ transition in ^{254}Rf. The $2^+ \rightarrow 0^+$ and $4^+ \rightarrow 2^+$ transitions have lower energies and undergo predominantly electron conversion. There are other clusters of counts in the spectrum but their firm assignment is difficult. In order to search for a rotational band in this low statistics spectrum a novel method was developed which takes advantage of the regular nature of rotational bands. Ground-state rotational bands in deformed even-even nuclei form a sequence of levels with even spins I=0,2,4,... and energies given by the formula:

$$E(I) = \frac{\hbar^2}{2\mathcal{J}} I(I+1), \qquad (1)$$

where $\mathcal{J}$ is the moment of inertia. The kinematic moment of inertia $\mathcal{J}^{(1)}$ can be expressed as a function of rotational frequency ω using the Harris formula [22]:

$$\mathcal{J}^{(1)} = \mathcal{J}_0 + \mathcal{J}_1 \omega^2, \qquad (2)$$

where $\mathcal{J}_0$ and $\mathcal{J}_1$ are the Harris parameters. The kinematic moment of inertia and the rotational frequency can be derived from the energies of γ-ray transitions $E_\gamma(I)$ in a rotational band using the expressions:

$$\mathcal{J}^{(1)} = (2I-1)/E_\gamma(I) \qquad (3)$$

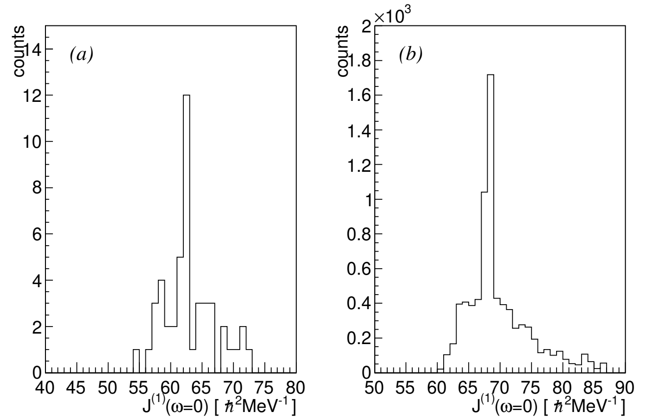

FIG. 4. Experimental moment of inertia (see text) calculated for the ground-state band in (a) ^{254}Rf and (b) ^{254}No.

and

$$\omega = E_\gamma(I)/2, \quad (4)$$

respectively. In order to search for a rotational band in the ^{254}Rf γ-ray spectrum, first, the spectrum was divided into 5 wide energy regions where individual ground-state band transitions starting with the $6^+ \rightarrow 4^+$ transition are expected to be located. For each γ-ray event (i) in region (j) the quantity:

$$\mathcal{J}_0^{exp}(i) = (2I(j)+1)/E_\gamma(i) - \mathcal{J}_1(E_\gamma(i)/2)^2, \quad (5)$$

corresponding to the $\mathcal{J}_0$ parameter was derived from eq. 2, where $I(j)$ is the spin assigned to region (j). The ^{254}Rf moment of inertia histogram calculated using the value of $\mathcal{J}_1$=211.2 $\hbar^2 MeV^{-3}$ derived from the fit to the ^{252}No ground-state rotational band is shown in Fig.4(a). A peak in such a spectrum indicates presence of a rotational band and its position represents the value of $\mathcal{J}_0$ for this band as illustrated in Fig. 4(b) where results of the same procedure applied to the ground-state rotational band in ^{254}No are shown. On further inspection, the peak in Fig.4 (a), which contains 15 counts including about 4 background counts, was formed by the clusters of counts at 384, 339, 285, 232, 172 keV, which are marked in Fig. 3. These clusters were interpreted as the $14^+ \rightarrow 12^+ \rightarrow 10^+ \rightarrow 8^+ \rightarrow 6^+ \rightarrow 4^+$ γ-ray sequence forming the ^{254}Rf ground-state rotational band. The 172, 232, 285, 339, 384 keV γ-ray energies were used to fit the Harris formula (eq. 2) and $\mathcal{J}_0 = 62.1$ $\hbar^2 MeV^{-1}$ and $\mathcal{J}_1 = 215.1$ $\hbar^2 MeV^{-3}$ parameters were found to fit the data best. The Harris formula results in the values of E(2$^+$)=48 keV and E(4$^+$)=158 keV for the lowest levels in the ^{254}Rf band. Similarily, the energies of 420 keV and 470 keV are predicted for the $16^+ \rightarrow 14^+$ and $18^+ \rightarrow 16^+$ transitions, respectively. Interestingly, 2 counts were registered at 470 keV in the ^{254}Rf spectrum.

TABLE I. Properties of ground-state rotational bands in even-even nuclei near Z=100, N=152 compared with results of microscopic-macroscopic calculations [7].

Isotope	E(2$^+$) keV	$\mathcal{J}_0$ $\hbar^2 MeV^{-1}$	$\mathcal{J}_1$ $\hbar^2 MeV^{-3}$	β_2^{calc}[7]	E$_{calc}$(2$^+$) [7] keV
^{254}Rf	48	62.1	215.1	0.247	46.9
^{252}No	46.4	64.4	211.2	0.249	44.5
^{250}Fm	44.0	68.1	233.0	0.248	43.9
^{256}Rf	44.8	66.7	179.7	0.249	43.4
^{254}No	44.1	68.2	160.0	0.252	41.6

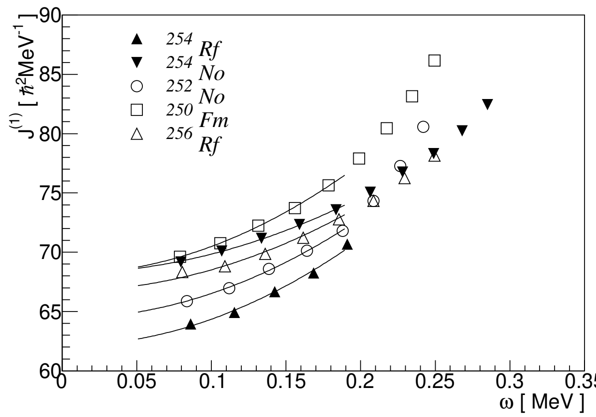

FIG. 5. Kinematic moments of inertia for N=150 and N=152 even-even isotones. The lines represent the Harris formula fitted to first 5 experimental points.

Discussion. The properties of the ground-state rotational bands in the even-even nuclei near Z=100 and N=152 including the new data for ^{254}Rf are shown in Table I. The experimental ground-state band kinematic moments of inertia as a function of rotational frequency for ^{254}Rf and neighboring nuclei is shown in Fig. 5. The curves in Fig. 5 represent fits to the Harris formula using the 6^+,...,14^+ levels. The value of $\mathcal{J}_0$ in ^{254}Rf, which corresponds to the moment of inertia at $\omega = 0$, is smaller than any of the $\mathcal{J}_0$ values deduced for the nuclei included in Fig. 5. A quadrupole deformation of β_2 =0.247 was calculated for ^{254}Rf using the microscopic-macroscopic model in Ref. [7]. This value is smaller than those calculated for all neighboring nuclei shown in Table I but this alone cannot explain the change in the moment of inertia. Compared to other nuclei, ^{254}Rf has more nucleons outside of the Z=100 and N=152 closed shells. This should result in stronger pairing correlations compared to other nuclei in Table I and lead to significant decrease of the moment of inertia. According to Ref. [7], the calculated energy of the 2^+ state derived from the rotational formula is 46.9 keV which agrees well with the value of 48 keV obtained from the $\mathcal{J}_0$ value deduced here. It is interesting to compare the microscopic-macroscopic approach

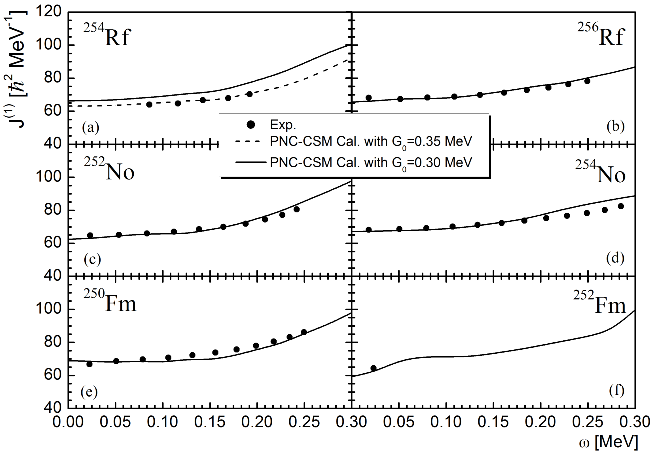

FIG. 6. The comparison between experimental kinematic moments of inertia and values calculated using the Particle-Number-Conserving Cranked Shell Model for N=150 and N=152 isotones of Fm, No and Rf. The experimental data are denoted by solid circles. The PNC-CSM calculations with pairing strengths $G_0 = 0.30$ and $G_0 = 0.35$ (only for ^{254}Rf) are shown as solid lines and a dashed line, respectively.

with self-consistent calculations. In Ref. [23], three different energy-density-functional (EDF) models, based on covariant, Skyrme, and Gogny functionals, each with two different parameter sets were used to calculate properties of trans-fermium nuclei including the kinematic moments of inertia (see Figs. 13 and 14 in Ref. [23]). Among the functionals used, only the D1M Gogny functional predicts the decrease of the moment of inertia in ^{254}Rf compared to ^{256}Rf and reproduces the experimental values well.

It is also interesting to inspect evolution of the moment of inertia with rotational frequency. The moment of inertia in ^{254}Rf increases with rotational frequency in a similar fashion as the lighter N=150 isotones and faster than in the N=152 isotones (see Fig. 5). The onset of alignment in the N=150 isotones was observed at around ω=0.2 MeV [18]. There is no evidence for alignment up to the maximum rotational frequency of 0.19 MeV observed in the present work.

Kinematic moments of inertia for N=150 and N=152 isotones of Fm, No and Rf calculated using the Cranked Shell Model with pairing treated by the Particle-Number-Conserving method are compared with the experimental values in Fig. 6. The calculated moments of inertia using a pairing strength of $G_0 = 0.30$, which are shown as solid lines, reproduce the experimental results very well for all nuclei except ^{254}Rf. The moment of inertia for ^{254}Rf is smaller than for the other nuclei which indicates stronger pairing correlations. The PNC-CSM calculations with a stronger pairing strength of $G_0 = 0.35$, which is denoted by the dashed line in Fig. 6, agrees very well with the experimental data in ^{254}Rf.

Summary. The ground-state rotational band was observed for the first time in the fissile nucleus ^{254}Rf. Levels up to spin $14\hbar$ and excitation energy of 1.56 MeV were identified. The moment of inertia deduced for ^{254}Rf is smaller than in neighboring nuclei. The moment of inertia is well reproduced by microscopic-macroscopic calculations whereas only the self-consistent approach with the D1M Gogny functional agrees with the data in ^{254}Rf and ^{256}Rf. The Particle-Number-Conserving Cranked Shell Model reproduces the kinematic moments of inertia as a function of rotational frequency for the N=150 and N=152 isotones of Fm, No and Rf except for ^{254}Rf where a larger moment of inertia is predicted. Good agreement between the calculations and the data was achieved for ^{254}Rf when the pairing strength was increased from $G_0 = 0.30$ to $G_0 = 0.35$.

In order to shed light on the rotational alignment in ^{254}Rf and competition between γ-ray emission and fission, more statistics are required to observe levels with higher spins at higher excitation energy. A search for a rotational band in the neighboring nucleus ^{250}No, which also decays rapidly by spontaneous fission, but can be produced with a larger cross section, should be also feasible.

This material is based upon work supported by the U.S. Department of Energy, Office of Science, Office of Nuclear Physics, under Contracts No. DE-AC02-06CH11357 (ANL) and DE-AC02-05CH11231 (LBNL) and by the National Natural Science Foundation of China under grant No. U2032138. This research used resources of ANL's ATLAS facility, which is a DOE Office of Science User Facility.

---

* seweryniak@anl.gov

[1] G. Münzenberg and K. Morita, Nuclear Physics A **944**, 3 (2015).
[2] Y. Oganessian and V. Utyonkov, Nuclear Physics A **944**, 62 (2015).
[3] K. Morita, Nuclear Physics A **944**, 30 (2015).
[4] A. Sobiczewski and K. Pomorski, Progress in Particle and Nuclear Physics **58**, 292 (2007).
[5] D. Ackermann and C. Theisen, Physica Scripta **92**, 083002 (2017).
[6] F. Al-Khudair, G.-L. Long, and Y. Sun, Phys. Rev. C **79**, 034320 (2009).
[7] A. Sobiczewski, I. Muntian, and Z. Patyk, Phys. Rev. C **63**, 034306 (2001).
[8] M. Bender, P. Bonche, T. Duguet, and P.-H. Heenen, Nuclear Physics A **723**, 354 (2003).
[9] A. V. Afanasjev, Physica Scripta **89**, 054001 (2014).
[10] H. L. Liu, F. R. Xu, and P. M. Walker, Phys. Rev. C **86**, 011301(R) (2012).
[11] Z.-H. Zhang, J. Meng, E.-G. Zhao, and S.-G. Zhou, Phys. Rev. C **87**, 054308 (2013).
[12] G. Ter-Akopyan, A. Iljinov, Y. Oganessian, O. Orlova, G. Popeko, S. Tretyakova, V. Chepigin, B. Shilov, and

G. Flerov, Nuclear Physics A **255**, 509 (1975).
[13] F. P. Heßberger, S. Hofmann, V. Ninov, P. Armbruster, H. Folger, G. Münzenberg, H. J. Schött, A. G. Popeko, A. V. Yeremin, A. N. Andreyev, and S. Saro, Zeitschrift für Physik A Hadrons and Nuclei **359**, 415 (1997).
[14] I. Dragojevic, K. E. Gregorich, C. E. Dullmann, M. A. Garcia, J. M. Gates, S. L. Nelson, L. Stavsetra, R. Sudowe, and H. Nitsche, Phys. Rev. C **78**, 024605 (2008).
[15] H. M. David, J. Chen, D. Seweryniak, F. G. Kondev, J. M. Gates, K. E. Gregorich, I. Ahmad, M. Albers, M. Alcorta, B. B. Back, B. Baartman, P. F. Bertone, L. A. Bernstein, C. M. Campbell, M. P. Carpenter, C. J. Chiara, R. M. Clark, M. Cromaz, D. T. Doherty, G. D. Dracoulis, N. E. Esker, P. Fallon, O. R. Gothe, J. P. Greene, P. T. Greenlees, D. J. Hartley, K. Hauschild, C. R. Hoffman, S. S. Hota, R. V. F. Janssens, T. L. Khoo, J. Konki, J. T. Kwarsick, T. Lauritsen, A. O. Macchiavelli, P. R. Mudder, C. Nair, Y. Qiu, J. Rissanen, A. M. Rogers, P. Ruotsalainen, G. Savard, S. Stolze, A. Wiens, and S. Zhu, Phys. Rev. Lett. **115**, 132502 (2015).
[16] J. L. Egido and L. M. Robledo, Phys. Rev. Lett. **85**, 1198 (2000).
[17] L. G. Moretto, L. Phair, and G. J. Wozniak, Phys. Rev. C **67**, 017301 (2003).
[18] P. T. Greenlees, J. Rubert, J. Piot, B. J. P. Gall, L. L. Andersson, M. Asai, Z. Asfari, D. M. Cox, F. Dechery, O. Dorvaux, T. Grahn, K. Hauschild, G. Henning, A. Herzan, R.-D. Herzberg, F. P. Hessberger, U. Jakobsson, P. Jones, R. Julin, S. Juutinen, S. Ketelhut, T.-L. Khoo, M. Leino, J. Ljungvall, A. Lopez-Martens, R. Lozeva, P. Nieminen, J. Pakarinen, P. Papadakis, E. Parr, P. Peura, P. Rahkila, S. Rinta-Antila, P. Ruotsalainen, M. Sandzelius, J. Saren, C. Scholey, D. Seweryniak, J. Sorri, B. Sulignano, C. Theisen, J. Uusitalo, and M. Venhart, Phys. Rev. Lett. **109**, 012501 (2012).
[19] J. E. Bastin, R.-D. Herzberg, P. A. Butler, G. D. Jones, R. D. Page, D. G. Jenkins, N. Amzal, P. M. T. Brew, N. J. Hammond, R. D. Humphreys, P. J. C. Ikin, T. Page, P. T. Greenlees, P. M. Jones, R. Julin, S. Juutinen, H. Kankaanpää, A. Keenan, H. Kettunen, P. Kuusiniemi, M. Leino, A. P. Leppänen, M. Muikku, P. Nieminen, P. Rahkila, C. Scholey, J. Uusitalo, E. Bouchez, A. Chatillon, A. Hürstel, W. Korten, Y. L. Coz, C. Theisen, D. Ackermann, J. Gerl, K. Helariutta, F. P. Hessberger, C. Schlegel, H. J. Wollerscheim, M. Lach, A. Maj, W. Meczynski, J. Styczen, T. L. Khoo, C. J. Lister, A. V. Afanasjev, H. J. Maier, P. Reiter, P. Bednarczyc, K. Eskola, and K. Hauschild, Phys. Rev. C **73**, 024308 (2006).
[20] R.-D. Herzberg, N. Amzal, F. Becker, P. A. Butler, A. J. C. Chewter, J. F. C. Cocks, O. Dorvaux, K. Eskola, J. Gerl, P. T. Greenlees, N. J. Hammond, K. Hauschild, K. Helariutta, F. Hessberger, M. Houry, G. D. Jones, P. M. Jones, R. Julin, S. Juutinen, H. Kankaanpaa, H. Kettunen, T. L. Khoo, W. Korten, P. Kusiniemi, Y. Le Coz, M. Leino, C. J. Lister, R. Lucas, M. Muikku, P. Nieminen, R. D. Page, P. Rahkila, P. Reiter, C. Schlegel, C. Scholey, O. Stezowski, C. Theisen, W. H. Trzaska, J. Uusitalo, and H. J. Wollersheim, Phys. Rev. C **65**, 014303 (2001).
[21] P. Reiter, T. L. Khoo, C. J. Lister, D. Seweryniak, I. Ahmad, M. Alcorta, M. P. Carpenter, J. A. Cizewski, C. N. Davids, G. Gervais, J. P. Greene, W. F. Henning, R. V. F. Janssens, T. Lauritsen, S. Siem, A. A. Sonzogni, D. Sullivan, J. Uusitalo, I. Wiedenhover, N. Amzal, P. A. Butler, A. J. Chewter, K. Y. Ding, N. Fotiades, J. D. Fox, P. T. Greenlees, R.-D. Herzberg, G. D. Jones, W. Korten, M. Leino, and K. Vetter, Phys. Rev. Lett. **82**, 509 (1999).
[22] S. M. Harris, Phys. Rev. **138**, B509 (1965).
[23] J. Dobaczewski, A. Afanasjev, M. Bender, L. Robledo, and Y. Shi, Nuclear Physics A **944**, 388 (2015).